1987ApJ...322..123L

THE ASTROPHYSICAL JOURNAL, 322:123–132, 1987 November 1
© 1987. The American Astronomical Society. All rights reserved. Printed in U.S.A.

THE EVOLUTION AND FINAL DISINTEGRATION OF SPHERICAL STELLAR SYSTEMS IN A STEADY GALACTIC TIDAL FIELD

HYUNG MOK LEE AND JEREMIAH P. OSTRIKER
Princeton University Observatory
Received 1986 March 28; accepted 1986 August 27

ABSTRACT

We have followed the dynamical evolution of simplified N-body systems in a steady galactic tidal field using an orbit-averaged Fokker-Planck code through the core collapse and quasi-static reexpansion phases. Assuming spherical symmetry and two mass categories, single stars and tidally captured binaries, and allowing interactions of binaries with singles and other binaries, we find that the mass of the cluster decreases linearly during the reexpansion phase until the cluster totally disintegrates in a finite time. A modified and we believe improved treatment of tidal losses is presented where mass loss is not instantaneous at the tidal radius. The main source of mass loss is "conductive flux" through the tidal boundary. The lifetime for total mass loss is found to be, aside from a slowly varying logarithmic term, proportional to the initial number of stars times the tidal time scale [$\sim 1/(G\rho_t)^{1/2}$], where ρ_t is the tidal density (i.e., mean density within the tidal radius). For a circular orbit around the galaxy (with flat rotation curve) our result could be restated as follows: the total lifetime of a cluster with short initial relaxation time is $\sim 5 \times 10^{-3} N$ orbital periods around the galaxy, where N is the initial number of stars in the cluster. The central part of the cluster is not significantly affected by the presence of the tidal limit until a substantial amount of the mass is lost. The dimensionless structure of the cluster follows a rather well defined one-parameter sequence similar to the King models. There are always King models having very similar surface density distributions to our appropriately scaled models. But the tidal radii of our postcollapse models are smaller than those of King models having similar surface density distributions by about a factor of 1.5. This would imply systematic error in mass estimates by about a factor of 3.5 if the galactic tidal field is used to determine the cluster mass.

Subject headings: clusters: globular — stars: stellar dynamics

I. INTRODUCTION

The early evolution of isolated globular cluster is now well understood. After an initial transient phase, the cores contract and the outer parts expand on the time scale of two-body relaxation, with the cluster passing through a sequence of more and more centrally concentrated states. After the central density exceeds the half mass density by a factor of $\sim 10^4$, which requires $\sim 14 t_{\mathrm{rh},i}$ (the relaxation time at half-mass point t_{rh} is defined in eq. [4.5] and the subscript i stands for the initial model), an accelerated gravothermal collapse will occur in a one-component system. In the absence of other energy inputs, a singular state is approached in a finite time, $\sim 15.8 t_{\mathrm{rh},i}$ (Cohn 1980). Note that the above time scales apply if the Plummer model is used as an initial model. Binaries or a spectrum of initial masses can only accelerate core collapse via the Spitzer (1969) mass stratification process as shown by Statler, Ostriker, and Cohn (1987; hereafter SOC), Applegate (1986), and Lee (1987).

However, central energy input can stop and reverse the collapse to a steady (but perhaps not stable) expanding phase, as envisioned by Henon (1961) in which the half-mass radius expands as $t^{2/3}$. Many physical processes have been proposed for central energy input (see Ostriker 1985), but binaries seem most promising either by direct heating effects or, indirectly, due to the mass loss they occasion. In any case, simulations passing through core collapse, bounce, and reexpansion phases have been carried out by Stodolkiewicz (1985), SOC, and Cohn and Hut (1985), the second utilizing close two-body tidal capture binaries, the third softer binaries made through the three-body process, and first utilizing both processes and several others in a more inclusive but less precise framework. All works find Henon's relation $r_h \propto t^{2/3}$ to be valid in the late phase for isolated clusters. Of the proposed origins for the binaries (initial, two-body, and three-body) it currently seems as if the two-body capture process and those that follow from it will be dominant, but (see McMillan 1986) more work must be done before a definite conclusion is possible.

Consequently, it is now necessary to look beyond core collapse to processes occurring during the reexpansion phase. It is obvious that clusters cannot expand according to Henon's prescription if they are limited by a tidal force field. Simple dimensional analysis (we are indebted to Piet Hut for contributing to the discussions here) and preliminary calculations (Stodolkiewicz 1985; Ostriker, Statler, and Lee 1984) show that one would expect the mass to decrease linearly with time in this phase, and it is useful to present the argument at this stage.

Core energy input will tend to adjust itself to equal the energy flow conducted via two-body relaxation at roughly the half-mass point. Thus the rate of expansion of an isolated system and, consequently, the rate at which a bounded system overflows its tidal limit is determined by the two-body relaxation rate at the half-mass point. The rate of evaporation $\dot{N}_{\mathrm{ev}}$ is thus

$$\dot{N}_{\mathrm{ev}} = -\mathrm{const}\ N/t_{\mathrm{rh}}\ , \tag{1.1}$$

where N is the total number of stars and t_{rh} is the relaxation time at half-mass point. Given the standard definition of relaxation time (eq. [4.5]), equation (1.1) can be written

$$N = \dot{N}_{\mathrm{ev}} = -\mathrm{const}\ (G\bar{\rho}_h)^{1/2} \ln (0.4N)\ , \tag{1.2}$$

© American Astronomical Society • Provided by the NASA Astrophysics Data System

1987ApJ...322..123L

where $\bar{\rho}_h$ is the mean density within the half-mass point. If the tidal field is steady, then we expect the cluster to be limited at a radius r_t defined so that $(N/r_t^3) \propto \rho_t$ is constant (see von Hoerner 1957). Using these ideas, Henon (1961) derived a self-similar solution for the evolution of tidally limited clusters; we may expect that a detailed treatment will resemble his idealized one in that $(\bar{\rho}_h/\rho_t)$ should be roughly constant. Then, since ρ_t is constant, the right-side of the equation (1.2) is a constant, aside from the slowly changing logarithm of the number of stars, and thus the number of stars will linearly go to zero on the time scale proportional to $(G\rho_t)^{-1/2}$. But the latter is proportional to $[GM_g(R)/R^3]^{-1/2}$ which is, in turn, proportional to the orbital period [here $M_g(R)$ is the galactic mass within the galactic orbital radius R of the cluster].

Thus it follows, from integrating equation (1.2), that a cluster will survive in this phase for a time proportional to the product of its orbital period around the galaxy and the number of stars it initially contains. This is one of the principal results of this paper.

While the presence of the galactic tidal field, which has been neglected in most previous works, does not much affect the central part of the cluster as long as the total mass remains a fair fraction of initial mass, it should determine the outer structure of the cluster. There are now three sources of mass loss; stars at high velocity tail of Maxwellian velocity distribution established through two-body relaxation (Spitzer 1940), the stars driven over the tidal boundary by the energy conducted to them (Henon 1961) and the ones escaping at high speed from the core due to superelastic collisions between binaries and singles, or binaries and other binaries (SOC).

It will be also interesting to derive the structure of the post-collapse clusters so that they can be compared with the observations. Most observed surface density distributions have been compared with the King (1966) models and are found to be in very good agreement up to a large fraction of tidal radius. The good agreement may reflect the fact that the globular clusters are usually dynamically well relaxed systems and King models should well represent such system. However, slight differences in the outer structure, where observations are difficult due to the very low surface brightness, may introduce large differences in the determination of tidal radius, and thereby the mean density. For a given tidal field we expect the outer structure of a globular cluster to be more populated than that of the King model in the same tidal field since the density at the tidal radius will not be exactly zero, as it is in the King model. The stars escape from the cluster in a finite time scale, which presumably is about the orbital time scale around the cluster. This leads to a significant change in the inferred tidal field, or for fixed tidal field, the inferred cluster mass, when compared to the King formulation.

The aim of this paper therefore is to develop detailed models of structures of globular clusters, especially in the postcollapse phase, following their dynamical evolution under the influence of a galactic tidal field. We assume a static tidal field, which is correct if the cluster moves in a circular orbit relative to the galactic center, for simplicity. We organize the paper in a following way: § II describes the initial models and model parameters. The computational details and assumptions made are described in § III, and the results are presented in § IV. Section V describes the evolution of cluster structures and compares with the King models. Section VI summarizes our basic conclusions and points out further work to be done.

II. INITIAL MODELS AND MODEL PARAMETERS

The clusters are assumed to be situated in an external tidal force field, which will induce a truncation in the cluster mass distribution, treated as spherically symmetric and defined by the equation

$$\boldsymbol{F}_t \equiv \frac{4\pi}{3} G\rho_t \boldsymbol{r} , \tag{2.1}$$

where $\boldsymbol{r}$ is the radial vector originating from the cluster center. We have chosen a Plummer density distribution ($n = 5$ polytrope) as an initial model. There is no tidal truncation initially. This is a conventional choice which has little effect on the final outcome of our calculations. The density profile of the Plummer model is

$$\rho(r) = \frac{3}{4\pi}\frac{M_i}{r_0^3}\frac{1}{[1 + (r/r_0)^2]^{5/2}} , \tag{2.2}$$

where r_0 is the scale length and M_i is the initial total mass of the cluster. The mass enclosed in a sphere of radius r is then

$$M(r) = M_i \frac{(r/r_0)^3}{[1 + (r/r_0)^2]^{3/2}} . \tag{2.3}$$

The initial tidal radius r_t, at which tidal force balances with the internal force, can be calculated for a given tidal density ρ_t, which remains constant throughout the evolution, by solving the relation

$$\rho_t \equiv \bar{\rho}(r_t) = \frac{M(r_t)}{(4/3)\pi r_t^3} , \tag{2.4}$$

to get

$$r_t = \left[\left(\frac{3M_i}{4\pi\rho_t r_0^3}\right)^{2/3} - 1\right]^{1/2} r_0 , \tag{2.5}$$

where $\bar{\rho}$ is the mean density of the cluster within tidal radius. The phase space density distribution function $f(E)$ of the Plummer model is simply a power law:

$$f(E) = \frac{24\sqrt{2}}{7\pi^3}\frac{r_0^2}{G^5 M_i^5} E^{7/2} , \tag{2.6}$$

where

$$E = \varphi - \frac{v^2}{2} ; \quad \nabla^2\varphi = +4\pi G\rho . \tag{2.7}$$

Note that the gravitational potential here has positive sign convention and vanishes at infinity.

To illustrate the results we have adopted physical units in which the initial cluster has $r_0 = 1.13$ pc and contains 3×10^5 stars, each of mass $m_* = 0.7\ M_\odot$ and radius $R_* = 0.57\ M_\odot$, as a standard model. The initial total mass is therefore $2.1 \times 10^5\ M_\odot$. These parameters are identical to SOC case, so that our results can be directly compared with theirs.

The tidal density for our standard run was chosen to be

$$\rho_t = 7 \times 10^{-7}\frac{M_i}{r_0^3}\ (\approx 0.1\ M_\odot\ \mathrm{pc}^{-3}) ,$$

which roughly corresponds to the Galactic tidal field at galactocentric distance of 8.3 kpc, when a flat rotation curve of 220 km s^{-1} for the Galaxy is assumed. The initial tidal radius in

© American Astronomical Society • Provided by the NASA Astrophysics Data System

1987ApJ...322..123L

this case is $r_t = 69.9r_0$, which is ~ 80 pc. We also used different values of ρ_t to confirm the scaling of $\dot{M} \propto (G\rho_t)^{1/2}$.

The most important dimensionless number controlling the time of core bounce, and thereby the structure of postcollapse evolution, is v_0/v_*, where v_* is the escape velocity at stellar surface and v_0 is the initial central velocity dispersion of the cluster. A higher number for this ratio gives a higher central density at reexpansion and more centrally concentrated surface density distributions for the postcollapse models. We have varied this ratio by varying r_0 from the standard model to get a wide range of postcollapse models as v_0 is scaled as $v_0 \propto r_0^{-1/2}$.

III. COMPUTATIONS

We have used the modified orbit-averaged Fokker-Planck code described in detail in SOC. This includes tidal capture binary formation and their interactions with single and other binaries. Both ejection and direct heating are explicitly included in the computations. We used the cross sections for tidal capture binary formation for an $n = 3$ polytropic model of Lee and Ostriker (1986), without taking some possible mergers among tidally captured pairs into account. Other cross sections for binary-single and binary-binary collisions are the same as in SOC. The SOC code is modified to accommodate the presence of galactic tidal field, as described below.

Our treatment of mass loss at or beyond the tidal loss is new. First, we calculate the tidal energy E_t [defined by the gravitational potential at the tidal radius with $\varphi(\infty) = 0$] at every potential recomputation step (every four Fokker-Planck steps) in an iterative way so that the mean density within the tidal radius remains constant. But we do not set the distribution function $f(E)$ to zero for $E \leq E_t$ for the simple reason that mass loss is not instantaneous at the tidal radius. Rather mass loss is zero there, since the tidal (eq. [2.1]) and the internal force just balance at that point. For larger radii (smaller energies) the loss time approaches the orbital time. The equation of motion outside the tidal boundary can be written

$$\frac{d^2\boldsymbol{r}}{dt^2} = \frac{4\pi}{3} G\rho_t \boldsymbol{r} - \frac{GM}{r^3}\boldsymbol{r}\,, \tag{3.1}$$

where we have assumed that the mass outside the tidal radius is negligible. By integrating the above equation and imposing the boundary condition $\dot{r} = 0$ at arbitrary point $r = r_S > (r_t)$, we get

$$\dot{x}^2 = \frac{4\pi}{3} G\rho_t \left(x^2 + \frac{2}{x} - x_S^2 - \frac{2}{x_S} \right), \tag{3.2}$$

where we have introduced dimensionless quantity $x(\equiv r/r_t)$. If we denote $x \equiv x_S(1 + \delta)$, the above equation can be rewritten

$$\dot{\delta} \propto \delta^{1/2} \left(1 - \frac{1}{x_S^3} \right)^{1/2}, \tag{3.3}$$

where we have assumed δ is small. The time scale required to double x from x_S (that is the time required to reach $\delta = 1$ from $\delta = 0$) can be obtained by integrating equation (3.3),

$$\Delta t \propto \left(1 - \frac{1}{x_S^3} \right)^{1/2}. \tag{3.4}$$

Then, taking $E \propto 1/x$, the above relation can be translated into the mass-loss rate

$$\frac{df(E)}{dt} = -\alpha f(E) \left[1 - \left(\frac{E}{E_t} \right)^3 \right]^{1/2} 2\pi \sqrt{\frac{4\pi}{3} G\rho_t}\,, \quad E \leq E_t\,, \tag{3.5}$$

where the constant α determines the efficiency of evaporation, which is presumably of order or less than unity, since the stars move in an orbital time scale around the cluster and therefore cannot escape faster than this time scale. Note that for $E = E_t$ the loss rate is zero rather than infinitely rapid as in the standard treatment. We have adopted $\alpha = 1$ in our study discussed below in detail, but we also report our results for $\alpha = 5$ and $\alpha = 0.2$ to show how sensitively the results depend upon α. The above formula ensures that the stars with $E \ll E_t$ leave from the cluster in a time scale of α times $P_{\rm orb}$, the orbital period of the stars near the tidal radius of the cluster.

IV. RESULTS

We have run our code as far as possible before being limited by increasing numerical errors. At the time of termination, $\sim 95\%$ of the initial mass has evaporated. We list some interesting physical parameters at three different epochs (initial, core collapse, and at the time when half of the initial mass remains) in Table 1. We also display the evolution of central density ρ_0 (Fig. 1*a*), central velocity dispersion v_0^2 (Fig. 1*b*), the core-radius (r_c), half-mass radius (r_h), and tidal radius (r_t) (Fig. 1*c*) in Figure 1 for the standard model. The clearest signature of the postcollapse models is the relatively low velocity dispersion. Note that the core radius is defined by

$$r_c^2 \equiv \frac{3v_0^2}{4\pi G\rho_0}\,, \tag{4.1}$$

as in King models. Also shown in this figure are the same quantities for an isolated cluster (no tidal cutoff) treated by SOC for comparison as dashed lines. The points in time at which the mass is reduced to half of the initial mass are indicated with arrows. It is evident that there is very little difference in the central conditions between these two cases until this time. The evolution of total mass contained within tidal radius is shown in Figure 2, which clearly indicates the linear decrease of mass in time during postcollapse phase as previously noted. Other results for α different from unity are also shown in this figure. Higher α gives more rapid mass loss than lower α. For $\alpha \to \infty$ our treatment approaches the conventional treatment of mass loss.

Following the discussion of § I, we write the evolution of

TABLE 1

PHYSICAL PARAMETERS AT THREE EPOCHS

Epoch	Initial	Peak	Half-Mass
$t/t_{\rm rh,i}$	0	15.2	432.8
t (yr)	0	3.14×10^9	8.94×10^{10}
ρ_0 ($M_\odot$ pc^{-3})	3.47×10^4	1.78×10^8	3.15×10^5
r_c (pc)	0.799	0.012	0.065
r_h (pc)	1.47	2.27	13.92
r_t (pc)	80	79	62
$v_r(0)$ (km s^{-1})[a]	11.6	12.6	0.73
N_b[b]	0	1078	173

[a] Line-of-sight central velocity dispersion.
[b] Total number of binaries.

© American Astronomical Society • Provided by the NASA Astrophysics Data System

1987ApJ...322..123L

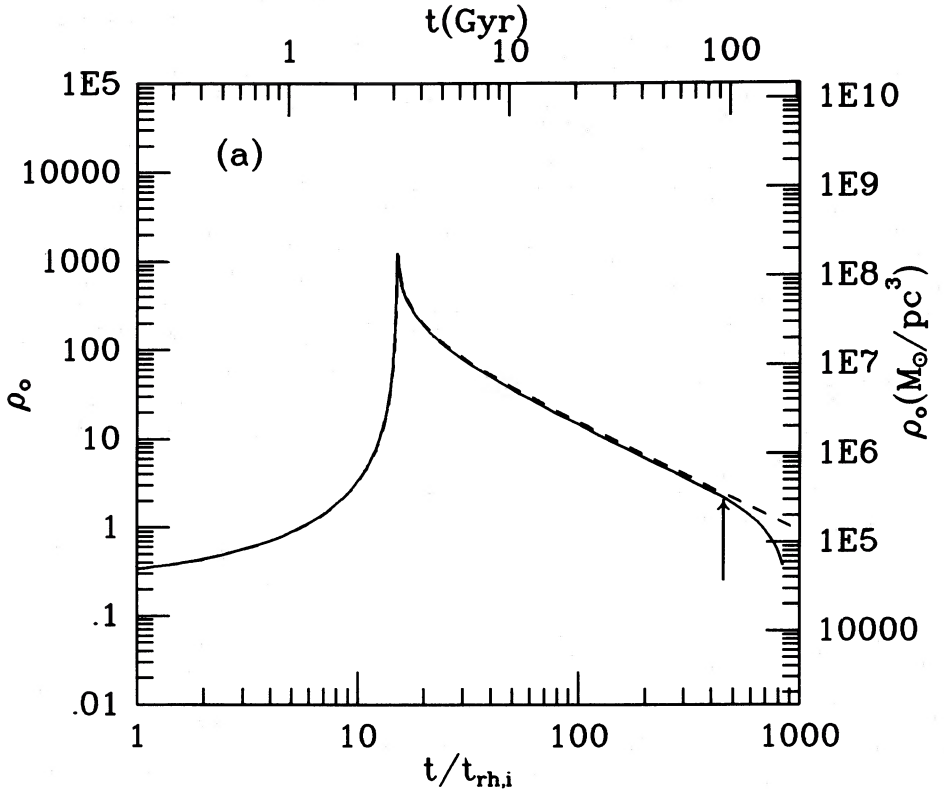

FIG. 1*a*

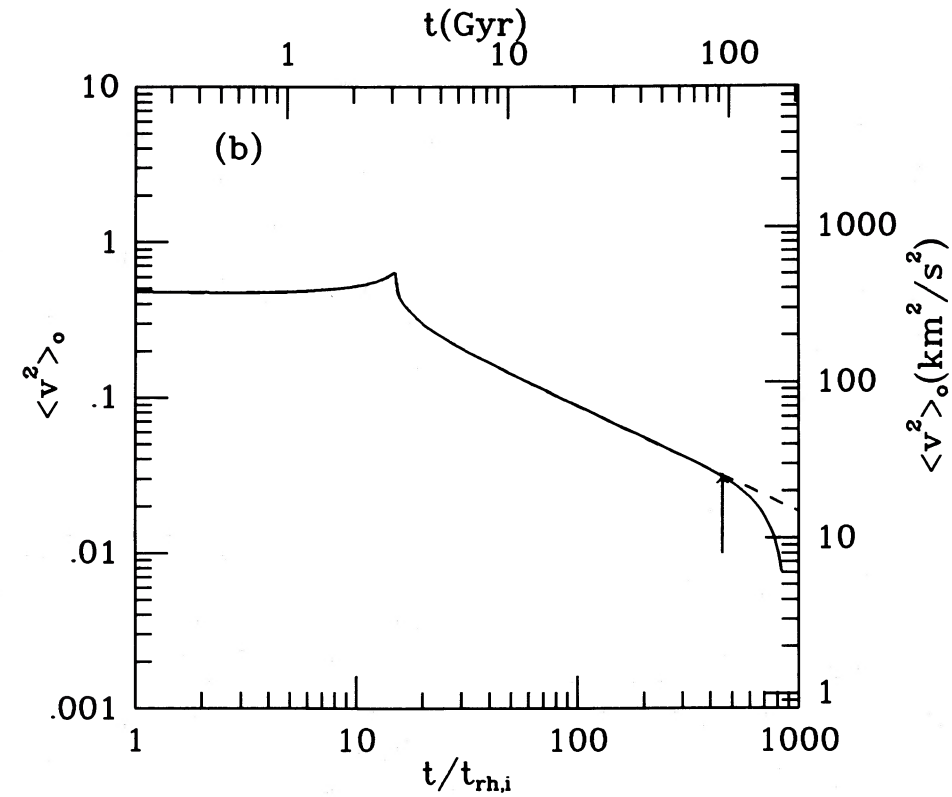

FIG. 1*b*

FIG. 1.—Evolution of (*a*) central density, (*b*) central velocity dispersion, and (*c*) core radius, half-mass radius, and tidal radius for an $\alpha = 1$ standard run. For comparison, same parameters for a run without a tidal cutoff are shown as dashed lines which begin to deviate from the solid lines at late stage. Arrows indicate the time when half of the cluster mass has evaporated.

© American Astronomical Society • Provided by the NASA Astrophysics Data System

1987ApJ...322..123L

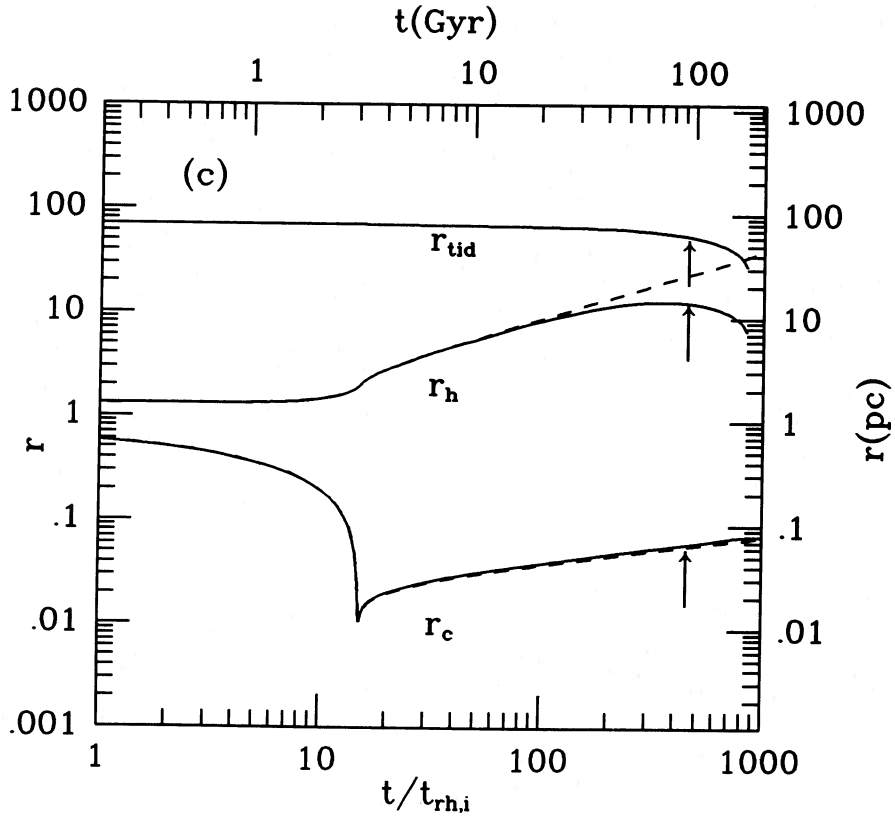

FIG. 1c

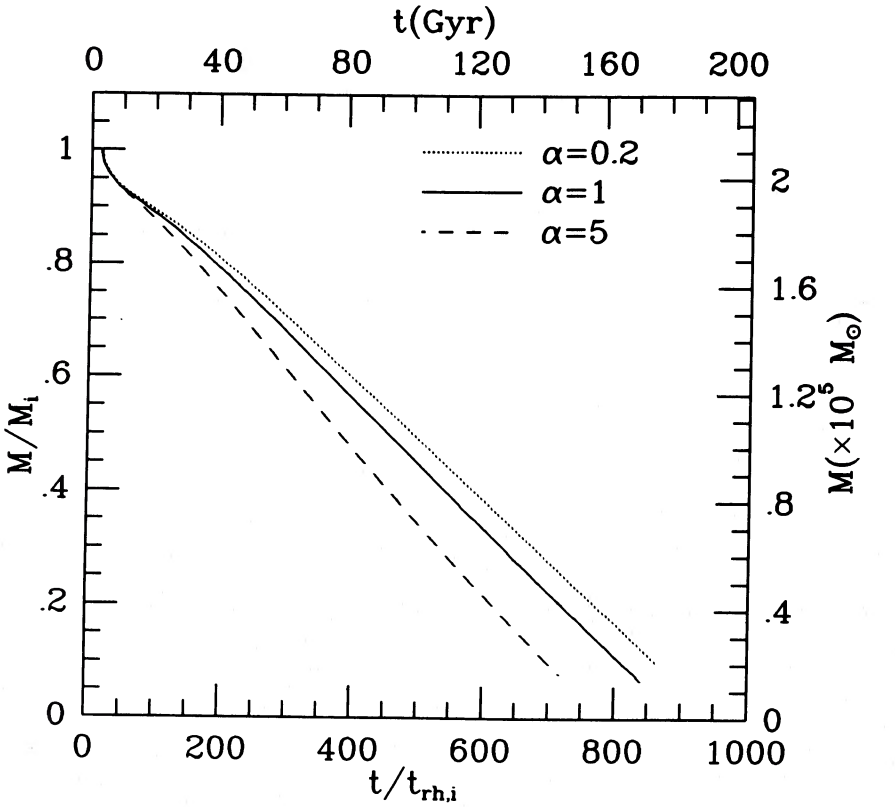

FIG. 2.—Evolution of total cluster mass as a function of time, which indicates a linear decrease of mass in time during postcollapse phase. Three different lines represent for the cases of $\alpha = 0.2$, 1, and 5.

© American Astronomical Society • Provided by the NASA Astrophysics Data System

1987ApJ...322..123L

mass during reexpansion as

$$M(t) \approx M_i(1 - \beta t) , \tag{4.2}$$

where t is the time elapsed from the core collapse, M_i is the initial cluster mass within tidal radius, β is a constant, and we define the evaporation time t_{ev} such that $M(t_{ev}) = 0$. Then one may write

$$t_{ev} = At_{tid} = Bt_{rh,i} , \tag{4.3}$$

where

$$t_{tid} \equiv 2\pi\left(\frac{4\pi}{3} G\rho_t\right)^{-1/2} \tag{4.4}$$

is a tidal time scale, $t_{rh,i}$ is the relaxation time at half-mass point of the initial model computed from (Spitzer and Hart 1971)

$$t_{rh,i} \equiv 0.135 \frac{N_i^{1/2} r_{h,i}^{3/2}}{m^{1/2} G^{1/2} \ln (0.4N_i)} , \tag{4.5}$$

and N_i is the initial total number of stars in the cluster. For a flat rotation curve t_{tid} is the orbital period of the cluster around the galaxy. The constants A and B can be found from the numerical results. From equation (4.4) the constant B can be determined utilizing the relation

$$B \propto \rho_t^{-1/2} , \tag{4.6}$$

which is also confirmed by the present numerical study. The constant B is found to be ~ 890 from the extrapolation of Figure 2 for the case of $\alpha = 1$. Now A can be written

$$A = \frac{Bt_{rh,i}}{t_{tid}} \approx 0.05 \frac{N_i}{\ln (0.4N_i)} , \tag{4.7}$$

so that the lifetime of a cluster becomes

$$t_{ev} \approx 0.05 N_i \frac{1}{\ln (0.4N_i)} t_{tid} , \tag{4.8a}$$

or for typical globular clusters ($N_i \approx 10^5$)

$$t_{ev} \approx 4.7 \times 10^{-3} P_{orb}$$
$$\approx 1.3\left(\frac{N_i}{10^5}\right)\left(\frac{R}{\text{kpc}}\right)\left(\frac{V_c}{220 \text{ km s}^{-1}}\right)^{-1} \times 10^{10} \text{ yr} , \tag{4.9}$$

so that the clusters initially having $\sim 10^5$ stars within 1 kpc from the Galactic center would have evaporated in a Hubble time. This is more or less consistent with the observed deficiency of globular clusters, relative to the spheroidal population stars, close to the Galactic center (Harris 1976). Although the sample of the globular clusters near the galactic center is incomplete because of heavy interstellar extinction, the relative deficiency is not dependent on the interstellar extinction. The evaporation time is proportional to the number of stars in the cluster, aside from a slowly varying $\ln (0.4N_i)$ term, times t_{tid}. There is $\sim 15\%$ difference in A between $\alpha = 1$ and $\alpha = 5$ cases. The deviation in A for $\alpha = 0.2$ from $\alpha = 1$ is smaller. As we argued in the previous section that α is expected to be order of unity or less, the estimate in lifetime t_{ev} is expected to be accurate within 10%. Also the structure of the cluster at any given cluster parameter (say, W_0) is even less sensitive to α. Most of our discussions in the followings are based on $\alpha = 1$ case.

It is instructive to compare our results with the Henon's (1961) homologous zero core radius model. He defined an escape probability

$$\xi_e \equiv -\frac{1}{t_{rh}} \frac{d \ln M}{dt} , \tag{4.10}$$

which was found to be a constant of 4.5×10^{-2} throughout the evolution. In Figure 3, we also plot our results for ξ_e as a function of time for $\alpha = 0.2$, 1, and 5 cases compared with Henon's constant value shown as a broken line. There is a large discrepancy between our results and those of Henon's just after core collapse, but the time-dependent results approach Henon's to within $\sim 20\%$ as evolution proceeds, and then in the final stage of the evolution the discrepancy becomes large again. This behavior can be understood as follows. The early pulse of energy released at core bounce has not reached tidal radius, so evaporation rate is less than Henon's, until the time when $t_r(0.5r_t) \approx 200t_{rh,i}$. Then it approaches the Henon's value. The differences in ξ_e among $\alpha = 0.2$, 1, and 5 cases are very small.

In a homologous model the mass-loss rate dM/dt must be, as we argued earlier, a constant. There is a close resemblance between our postcollapse models and the homologous model since the core radius of postcollapse cluster is usually very small compared to any other radius (i.e., half-mass radius or tidal radius). This fact produces the approximately constant mass-loss rate in our model.

In Figure 4, we show each component of the mass-loss rate as a function of time. Ejection from the core, which accounts for most of the mass loss during precollapse and very brief postcollapse phase just after core collapse, is due to stars escaping because of the high energy gained by binary-single or binary-binary encounters. "Conductive flux," on the other hand, is due to the stars near tidal boundary which happens to gain enough energy to overcome the tidal energy barrier due to the general outflow originating from the core. It is evident that the "conductive flux" accounts for most of the mass loss during later evolution and is almost a constant.

V. COMPARISONS OF POSTCOLLAPSE MODELS WITH KING MODELS

To study the evolution of the structure of the cluster, we pick out the surface density distributions at several epochs during the postcollapse evolution. Cohn (1980) noted that a good agreement between models derived from single-component dynamic calculations using an orbit averaged Fokker-Planck code and King models for the early precollapse stage up to a large radius. We make some detailed comparisons between our postcollapse models and King models in this section.

The parameter determining the structure of a dimensionless surface density distribution in the King model is the scaled central potential W_0 ($\equiv 3[\varphi_0 - \varphi_t]/v_0^2$), where φ_0 and φ_t are gravitational potential at the center and tidal radius, respectively. In our computed model, W_0 is a monotonically decreasing function of time during the postcollapse evolution. Other parameters characterizing the structure of the cluster are half-mass radius r_h, core radius r_c, and tidal radius r_t. We also introduce the de Vaucouleurs effective radius r_e within which half of the total projected density (or light) is enclosed, since this might be easier to determine observationally than any of the parameters listed above.

To compare the structures between our postcollapse and the King model, we normalize the surface density distribution by

© American Astronomical Society • Provided by the NASA Astrophysics Data System

1987ApJ...322..123L

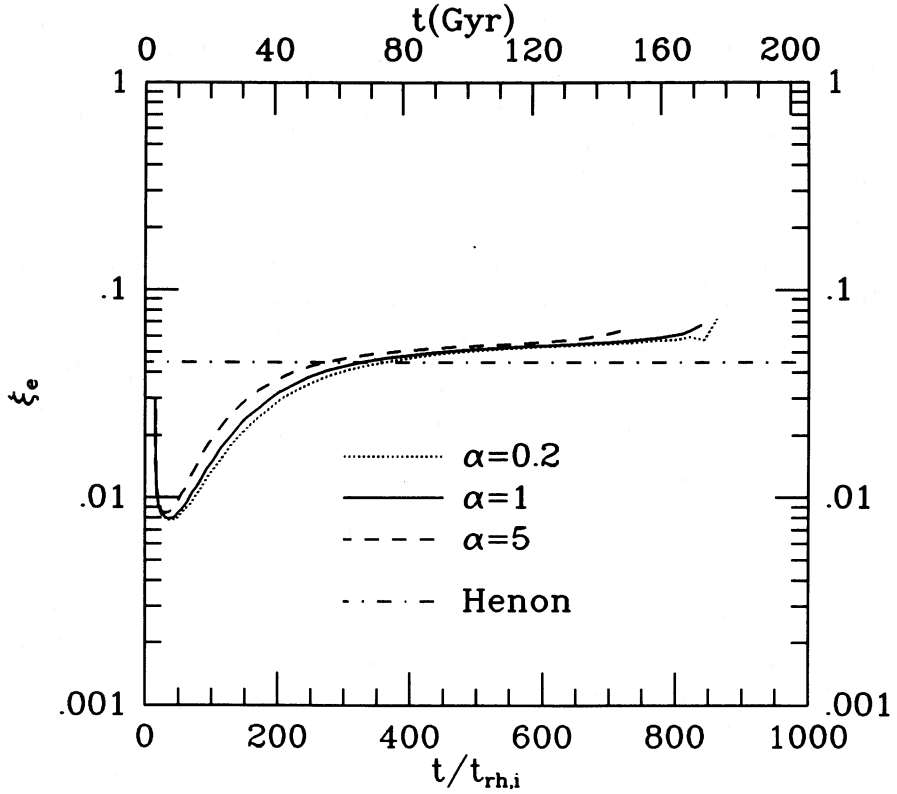

FIG. 3.—Escape probability defined by eq. (4.10) as a function of time during reexpansion phase for $\alpha = 0.2$, 1, and 5. For comparison, Henon's constant of $\xi_e = 0.045$ is also shown.

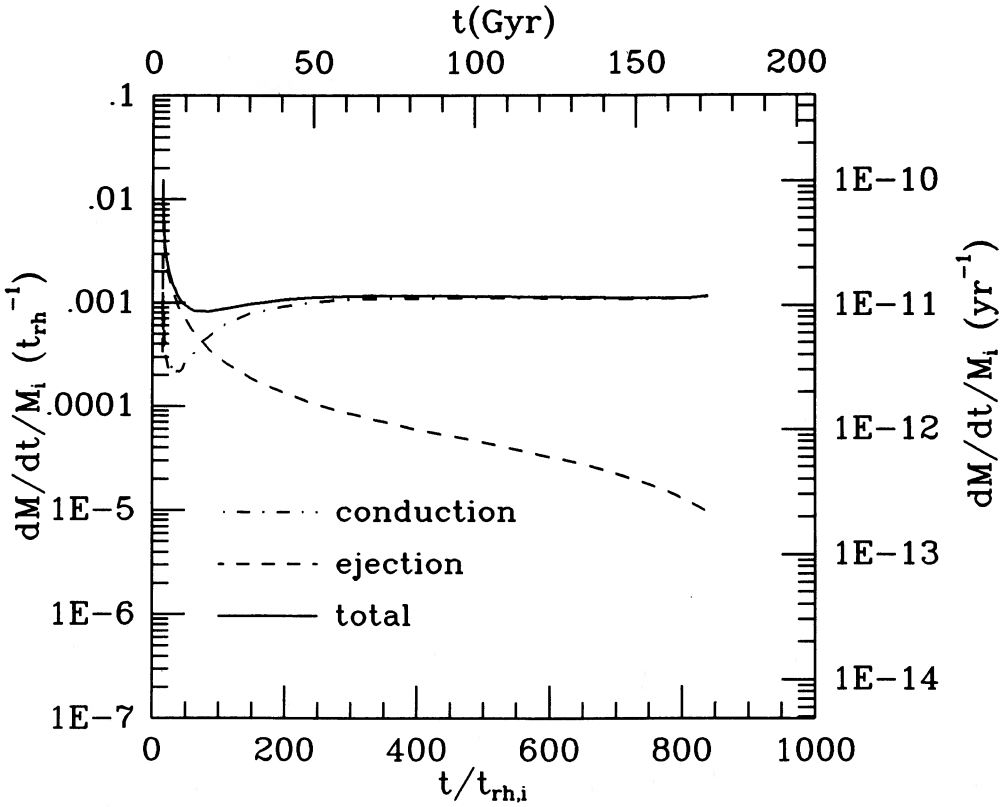

FIG. 4.—Mass-loss rates for different sources. Ejection is due to high-velocity stars which gained their high energy involving binaries near the center, while "conduction" is due to general outflow of mass which is a result of the expansion.

© American Astronomical Society • Provided by the NASA Astrophysics Data System

1987ApJ...322..123L

the central surface density and the projected radius by the effective radius r_e. An example of the postcollapse model is shown in Figure 5, together with a King model having same total mass (or total luminosity), same central surface density (or central surface brightness), and same effective radius. (In fact, the latter two are automatically satisfied by the normalization.) We mark the locations of the core radius (defined by eq. [4.1]), which is very close to the radius where surface brightness is half of the central value, and the tidal radius. Please remember that our definition of tidal radius is the radius where the tidal force and the internal force balance (see eq. [2.1]) as opposed to the usual definition of the place where the density goes to zero. A very close similarity in surface density distribution between our postcollapse model and a King model is evident from Figure 5 except for the somewhat different locations of core and tidal radii. For each postcollapse model a King model can be found which has a very similar surface density distribution and the same total luminosity, central surface density, and effective radius.

We display a whole sequence of normalized surface density distribution obtained from three runs with different r_0's (1.13, 0.565, and 0.226 pc) in Figure 6 so that the theoretical curve can be used to compare with observed surface brightness distribution. The parameters characterizing each model are summarized in Table 2 in comparison with the King models. Note that we have parameterized our models by a dimensionless number which may be determined from observations

$$P_0 \equiv r_e/(L_{\rm tot}\,\sigma_c)^{1/2}\,, \tag{5.1}$$

TABLE 2

MODEL PARAMETERS FOR SURFACE DENSITY DISTRIBUTION

$P_0 \equiv r_e/(L_{\rm tot}/\sigma_c)^{1/2}$	W_0	W_0 (King)	r_e/r_c	r_e/r_c (King)	r_t/r_c	r_t/r_c (King)
3.14	13.8	10.30	36.0	27.1	215	258
4.48	14.1	11.78	70.4	57.5	406	497
5.81	15.5	13.11	121.1	103.6	707	906

where $L_{\rm tot}$ is the total luminosity (or mass) and σ_c is the central surface brightness (or projected mass density). We also show the dependences of r_e and r_t on P_0, together with the King sequence. It is clear that P_0 is a good parameter for characterizing the surface density distribution.

The mass of the cluster $M_{\rm cl}$ can be determined, if the galactic tidal field (i.e., ρ_t) is known, using the relation

$$M_{\rm cl} = \tfrac{4}{3}\pi r_t^3 \rho_t\,. \tag{5.2}$$

The tidal radius can be easily obtained from Figure 7 if P_0 is known. Many observed clusters are less concentrated than our models. This is probably due to the fact that they have not reached through core collpase and bounce phases. But if some mechanism to make the cluster begin reexpansion at lower central density is found, we can extend P_0 to smaller values to allow comparison with many more clusters.

As evident from the Table 2 and Figure 7, our r_t/r_e's are smaller than those of King models having similar surface density distribution by about a factor of 1.5–1.6. This means

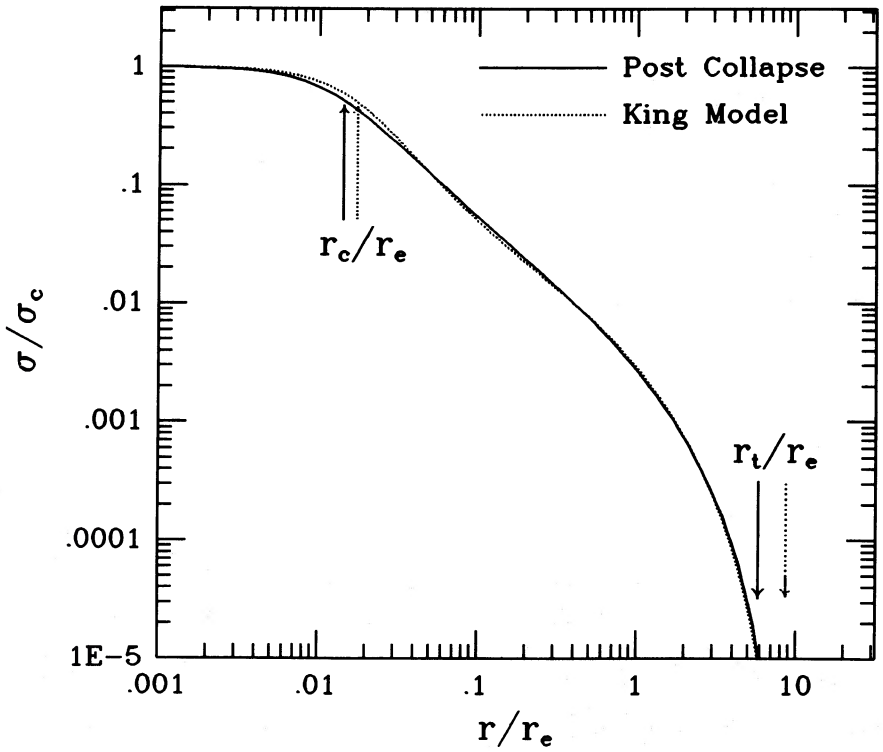

FIG. 5.—Example of normalized surface density distribution of one of the present postcollapse model compared with the King model having same total luminosity, same effective radius, and same central surface brightness. The radius is normalized by the de Vaucouleurs effect radius r_e, within which half-light is contained, instead of core radius r_c, since the former is more clearly defined observationally. Note the different locations of tidal and core radii between these two models.

© American Astronomical Society • Provided by the NASA Astrophysics Data System

1987ApJ...322..123L

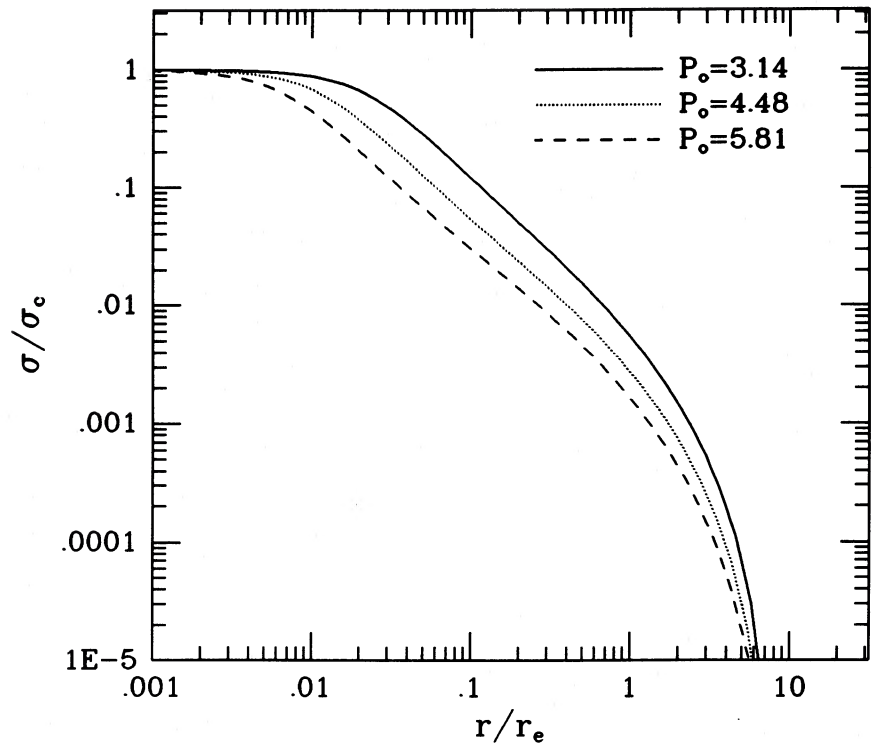

FIG. 6.—Sequence of surface density distribution of postcollapse models obtained from three runs with different values of r_0, the length scale of the initial model. These three models are those listed in Table 2.

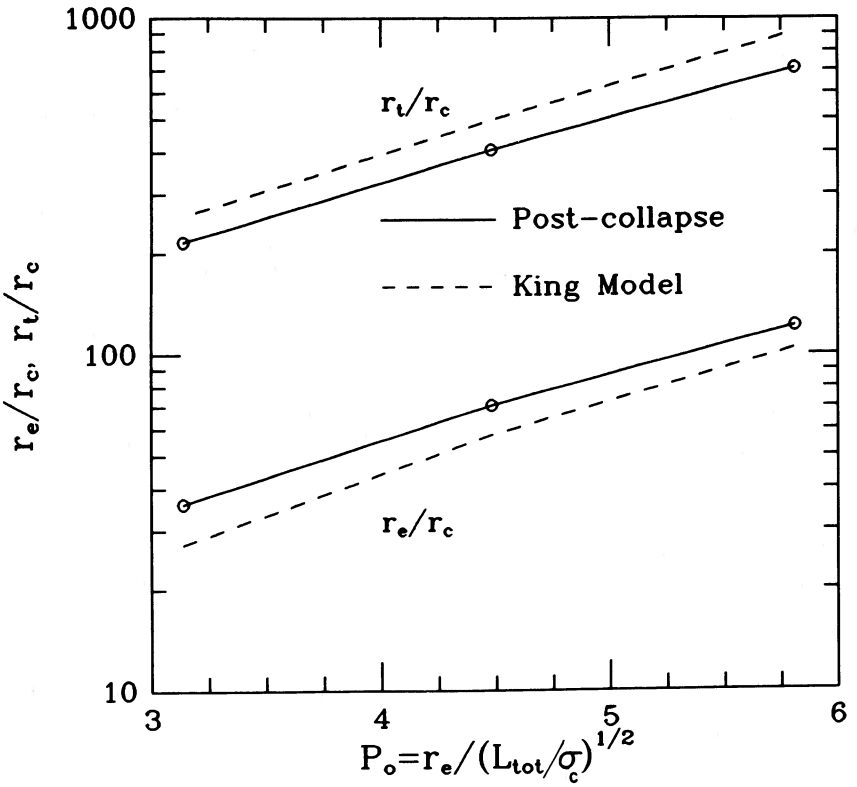

FIG. 7.—Dependence of r_e/r_c and r_t/r_c on the dimensionless parameter P_0 defined by eq. (5.1) for postcollapse models (*solid lines*). Open circles indicate the three models shown in Fig. 7 and Table 2. The tidal radii in units of effective radius do not vary from model to model because of the similar slopes for r_t/r_c and r_e/r_c. Note that r_t/r_e is larger in our collapse model by about a factor of 1.5–1.6 than in the King models for a given P_0.

© American Astronomical Society • Provided by the NASA Astrophysics Data System

1987ApJ...322..123L

that the tidal radii derived by fitting the observed surface brightness to the theoretical surface density distribution will be smaller by the same factor depending on the theoretical curve used. This implies the possible overestimate of M_{cl} by about a factor of 3.4–4 if equation (3.5) is used to compute the cluster mass with r_t determined by using the King model. We note here that the mass-to-light ratio for globular clusters varies only within $\sim 30\%$ (Pryor, McClure, and Hesser 1985) so that the systematic errors in r_t can be much more significant than the random errors in the mass estimates.

VI. DISCUSSION

Energy input from the postcollapse globular clusters will diffuse through the clusters, and, as it reaches the outer parts, it will drive matter over the tidal limit and ultimately cause the total disintegration of the cluster in a finite time. If our results are translated to astronomical units (eq. [4.9]), we see that a typical low-mass cluster ($M \lesssim 10^5\ M_\odot$) orbiting within 1 kpc of the Galactic center should have been destroyed in a Hubble time by this process. Coincidently, this is approximately the Galactic radius at which Tremaine, Ostriker, and Spitzer (1975) found the massive globular clusters ($M \gtrsim 10^5\ M_\odot$) would be removed by dynamical friction. The two processes are complementary and thus may explain the relative depletion of globular clusters, compared with spheroidal population stars within 1 kpc of the Galactic center.

Second, we have presented a new way of treating the rate of mass loss near the tidal radius, taking it to be zero at the place where the forces balance and approaching the dynamical time scale beyond the tidal radius. For a given external tidal field and observed cluster surface distribution, the internal cluster mass derived is *smaller* by a factor of 3.4–4 than with King models.

Many questions arise concerning the validity of our treatment. Let us address some of the most obvious issues. We adopted a specific model for energy input due to tidally produced binaries. Would the results have been different if another energy input has been used? In detail the results would certainly have been different, particularly with respect to the core properties. But we expect that the mass versus time relation would not be changed very much. For example, in a run with the tidal capture cross section doubled over the standard case, t_{ev} was decreased by less than 2%. This is because central conditions will always adjust to give the same half-mass conductive luminosity, analogous to the result in stellar structure that luminosity is surprisingly insensitive to nuclear cross sections.

Next we consider our assumption of velocity anisotropy. Spitzer and Shapiro (1972) have shown that, in the halo of an isolated cluster, the orbits become increasingly radial and a density distribution $\rho \propto r^{-3.5}$ will be set up through the dynamical evolution. This would seriously alter the results for evaporation over a tidal boundary. However, there are two processes acting which may tend to isotropize the orbits in the outer parts of the cluster. The tidal force itself (King 1974) and the tidal shocks (Ostriker, Spitzer, and Chevalier 1972; Chernoff, Kochanek, and Shapiro 1986) due to crossing the Galactic plane could tend to isotropize orbits in the outer part of the clusters by selectively removing stars with radial orbits. A very rough perusal of these processes indicates that they are likely to be efficient in preventing the establishment of a radial velocity distribution.

Is a steady, spherically symmetric tidal force sensible? Clearly not for clusters on elongated Galactic orbits, but we may hope that, for an appropriately weighted average value of ρ_t, our treatment should give reasonable results.

Finally let us turn to the question of the effects of tidal shocks. It seems that these could quite change the structure in the outer parts of the cluster and simultaneously reduce the evaporation time. We will return to this topic in another paper.

We would like to thank T. Statler, D. Heggie, and L. Spitzer for useful remarks, and the NSF for material support through a grant AST 83-41412. H. M. L. thanks the Korean Ministry of Education for a Graduate Scholarship.

REFERENCES

Applegate, J. 1986, *Ap. J.*, **301**, 132.
Chernoff, D. F., Kochanek, C. S., and Shapiro, S. L. 1986, *Ap. J.*, **309**, 183.
Cohn, H. N. 1980, *Ap. J.*, **242**, 765.
Cohn, H. N., and Hut, P. 1985, *Bull. AAS*, **17**, 603.
Harris, W. E. 1976, *A.J.*, **81**, 1095.
Henon, M. 1961, *Ann. d'Ap.*, **24**, 369.
King, I. R. 1966, *A.J.*, **71**, 64.
———. 1974, in *IAU Symposium 69, Dynamics of Stellar Systems*, ed. A. Hayli (Dordrecht: Reidel), p. 99.
Lee, H. M. 1987, *Ap. J.*, **319**, 801.
Lee, H. M., and Ostriker, J. P. 1986, *Ap. J.*, **310**, 176.
McMillan, S. L. W. 1986, *Ap. J.*, **306**, 552.
Ostriker, J. P. 1985, in *IAU Symposium 113, Dynamics of Star Clusters*, ed. J. Goodman and P. Hut (Dordrecht: Reidel), p. 347.
Ostriker, J. P., Spitzer, L., Jr., and Chevalier, R. A. 1972, *Ap. J. (Letters)*, **176**, L51.
Ostriker, J. P., Statler, T. S., and Lee, H. M. 1984, *Bull. AAS*, **16**, 946.
Pryor, C. P., McClure, R. D., and Hesser, J. E. 1985, *Bull. AAS*, **17**, 802.
Spitzer, L., Jr. 1940, *M.N.R.A.S.*, **100**, 397.
———. 1969, *Ap. J. (Letters)*, **158**, L139.
Spitzer, L., Jr., and Hart, M. H. 1971, *Ap. J.*, **166**, 483.
Spitzer, L., Jr., and Shapiro, S. L. 1972, *Ap. J.*, **173**, 529.
Statler, T. S., Ostriker, J. P., and Cohn, H. N. 1987, *Ap. J.*, **316**, 626 (SOC).
Stodolkiewicz, J. 1985, in *IAU Symposium 119, Dynamics of Star Clusters*, ed. P. Hut and J. Goodman (Dordrecht: Reidel), p. 361.
Tremaine, S., Ostriker, J. P., and Spitzer, L., Jr. 1975, *Ap. J.*, **196**, 407.
von Hoerner, S. 1967, *Ap. J.*, **125**, 451.

HYUNG MOK LEE: Canadian Institute for Theoretical Astrophysics, McLennan Physical Laboratories, University of Toronto, Toronto, Ontario M5S 1A1, Canada

JEREMIAH P. OSTRIKER: Princeton University Observatory, Peyton Hall, Princeton, NJ 08544

© American Astronomical Society • Provided by the NASA Astrophysics Data System